Dynamic Nonisothermal Transport in Hygroscopic Porous Media: Moisture Diffusion in Wood

Stavros Avramidis
Harvesting and Wood Science Dept., University of British Columbia, Vancouver, B. C., Canada V6T1Z4

Peter Englezos
Pulp and Paper Centre, Chemical Engineering Dept., University of British Columbia, Vancouver, B. C., Canada V6T1Z4

Thanasis Papathanasiou
Mechanical and Electronics Engineering Division, Los Alamos National Laboratory, Los Alamos, NM 87545

A model that predicts heat and moisture transfer in the hygroscopic range of a complex porous material such as wood, was evaluated with unsteady-state nonisothermal diffusion experimental data. Water chemical potential gradient was taken as the driving force for diffusion, and the derivation of the temperature-gradient phenomenological coefficient in the mass balance equation was based on the principles of nonequilibrium thermodynamics. The results reveal an excellent prediction of the specimen's average moisture content during desorption in the hygroscopic range. Moreover, a very good agreement was also shown between the specimen's center temperature and the model predictions. The model revealed the existence of a thermal-diffusion phenomenon during the initial stages of the desorption process. This phenomenon was not predicted by Fick's equation for diffusion.

Introduction

Because of its important applications in the chemical industry, coupled heat and mass transfer in porous macromolecular solids arouses great interest within the chemical engineering field. Some of the fields that have to gain from an expansion of our understanding regarding the interaction of heat and mass transfer in complex porous materials are the drying of foods (Parry, 1985; Haghighi et al., 1990); the drying of wood and ceramics (Stanish et al., 1984, 1986); the diffusion of solvents in polymers (Laubi and Vergnaud, 1991), with obvious applications in devolatilization (Maffettone et al., 1991); the moisture absorption in fiber-reinforced plastics with aerospace and other demanding structural applications (Collins, 1991); the study of mechanical deterioration of materials during drying or in-service (Lewis et al., 1976; Jomaa and Puiggali, 1991). Models that adequately describe mass and heat transfer in such media, can be used to study and evaluate alternative industrial processing schemes, to facilitate experimental testing, and to explain the physical mechanisms responsible for those particular transport processes.

A considerable volume of research has been carried out in modeling heat and moisture transfer in materials such as polymers, wood, soils, coatings, and agricultural products (Parrouffe and Mujumdar, 1988; Perre et al., 1986; Parry, 1985; Strongin and Border, 1986; Oliveira and Fernandes, 1986; Croll, 1987; Blondin et al., 1987). Using wood as the porous hygroscopic material, model developments have been based on either mechanistic approaches in which, macroscopic descriptions of transfer phenomena have been derived from Fourier's and Fick's laws, or on the principles of nonequilibrium thermodynamics. The latter embodies the entropy production and flow in an open system that can identify the driving forces and relate them to the heat and moisture fluxes through a number of phenomenological coefficients (Stanish et al., 1984, 1986; Plumb et al., 1984; Beard et al., 1983; Thomas et al., 1980; Adesanya et al., 1988; Bramhall, 1979a,b; Liu, 1990; Kayihan, 1986; Avramidis and Siau, 1987b).

There is a conspicuous absence in the literature of models that describe moisture fluxes and profiles in wood under dynamic, nonisothermal conditions. This can be explained by the sorption of moisture always being accomplished either by evolution or by the absorption of heat. The heat conducts through the material and causes temperature fluctuations. As a result, the material's ability to adsorb or desorb moisture is affected. Consequently, heat and moisture transfer should be considered

coupled processes. The thermally induced mass transfer (Soret effect), which contributes considerably to the total moisture flux, should always be taken into account (Philips and DeVries, 1957; DeGroot and Mazur, 1962; Prigogine, 1961; Fortes and Okos, 1978). Traditionally, moisture content gradients have been employed as the driving forces for diffusion (Droin et al., 1988; Droin-Josserand et al., 1988, 1989a,b; Vergnaud, 1991). In addition, the gradients of water chemical potential, partial and spreading pressures have also been used (Nelson 1986a,b,c; Siau, 1983b, 1984a,b).

In a previous study, a new form of the phenomenological coefficient, which describes the direction and magnitude of moisture fluxes through a hygroscopic porous material, was proposed, and the derived model was evaluated under steady-state nonisothermal conditions (Avramidis et al., 1987; Avramidis and Siau, 1987b; Siau et al., 1986; Siau and Avramidis, 1992). In this study, we will formulate and evaluate a set of coupled partial differential equations that utilize this phenomenological coefficient. This model is expected to simulate unsteady-state nonisothermal moisture diffusion and heat transfer in the hygroscopic range of a complex porous and hygroscopic material.

Model Development

According to the principles of nonequilibrium thermodynamics, NET, (Prigogine, 1961; Luikov, 1966), the general equations that describe one-dimensional heat and moisture transfer in a porous hygroscopic material with no free water present in the pores have the following form:

$$J_m = L_{mq}\frac{\partial T}{\partial x} + L_{mm}\frac{\partial M}{\partial x} \tag{1}$$

and

$$J_q = L_{qq}\frac{\partial T}{\partial x} + L_{qm}\frac{\partial M}{\partial x} \tag{2}$$

where J_m and J_q are the moisture and heat fluxes, respectively and the quantities L_{mq}, L_{mm}, L_{qm}, and L_{qq}, are the phenomenological coefficients. In a previous series of studies (Avramidis and Siau, 1987b; Siau and Avramidis, 1992), new expressions for the phenomenological coefficients of Eq. 1, were proposed. The calculated moisture fluxes were successfully compared with the experimental data obtained for wood under steady-state nonisothermal conditions. The moisture "flux reversal" phenomenon was also effectively predicted. The temperature gradient coefficient was given as:

$$L_{mq} = K_M\left(\frac{H}{RT}\right)\left(\frac{\partial M}{\partial H}\right) \times \left[\frac{d\mu^o}{dT} + \frac{E_o + E_b + E_1}{T} + \mathrm{Rln}\left(\frac{H_{p_o}}{7{,}600}\right)\right] \tag{3}$$

and was named the "chemical potential" or CP coefficient, because its derivation was based on the assumption that the water chemical potential gradient is the driving force for diffusion. Furthermore, it was assumed that the thermal heat of transfer, which is the total energy transported by a water molecule less its enthalpy (Oriani, 1961), is equal to the activation energy for diffusion. The entropy production and flow in an open system was also considered in deriving L_{mq} (Avramidis and Siau, 1987b). The phenomenological coefficient for the moisture gradient is:

$$L_{mm} = K_M = \frac{G\rho D}{100} \tag{4}$$

The single-component moisture conservation equation without chemical reaction (Siau, 1983a) is given by:

$$\frac{\partial M}{\partial t} = D\left(\frac{\partial^2 M}{\partial x^2}\right) + \left(\frac{\partial D}{\partial M}\right)\left(\frac{\partial M}{\partial x}\right)^2 + \left(\frac{\partial \phi}{\partial M} + \frac{\partial D}{\partial T}\right)\left(\frac{\partial M}{\partial x}\right)\left(\frac{\partial T}{\partial x}\right) + \left(\frac{\partial \phi}{\partial T}\right)\left(\frac{\partial T}{\partial x}\right)^2 + \phi\left(\frac{\partial^2 T}{\partial x^2}\right) \tag{5}$$

where

$$\phi = \left(\frac{d\mu^o}{dT} + \frac{E_o + E_b + E_L}{T} + \mathrm{Rln}\left(\frac{H_{p_o}}{7{,}600}\right)\right)\left(\frac{DH}{RT}\right)\left(\frac{\partial M}{\partial H}\right) \tag{6}$$

When ϕ is multiplied by $G\rho/100$, it yields the phenomenological coefficient L_{mq} of Eq. 1. By taking the derivatives of $\phi = f(M, T)$ with respect to moisture content and temperature, we obtain:

$$\frac{\partial \phi}{\partial M} = \left(\frac{H}{RT}\right)\left(\frac{\partial M}{\partial x}\right)\left(\frac{\partial D}{\partial x}\right)\theta + \frac{D\theta}{RT} + \left(\frac{DH}{RT}\right)\left(\frac{\partial M}{\partial H}\right)\left(\frac{-70 - 700\exp(-0.14M)}{T} + \frac{R}{H}\frac{\partial H}{\partial M}\right) \tag{7}$$

and

$$\frac{\partial \phi}{\partial T} = \left(\frac{H\theta}{RT}\right)\left(\frac{\partial M}{\partial H}\right)\left(\frac{\partial D}{\partial T}\right) + \left(\frac{D}{RT}\right)\left(\frac{\partial H}{\partial T}\right)\theta - \left(\frac{D}{RT^2}\right)\left(\frac{\partial M}{\partial H}\right)\theta + \left(\frac{DH}{RT}\right)\left(\frac{\partial M}{\partial H}\right)\left[0.0077 + \frac{70M - 5{,}000\exp(-0.14M) - 22{,}660}{T^2} + \left(\frac{R}{H}\right)\left(\frac{\partial H}{\partial T}\right) + \frac{10{,}400}{T^2}\right] \tag{8}$$

where

$$\theta = \frac{d\mu^o}{dT} + \frac{E_0 + E_L + E_b}{T} + \mathrm{Rln}\left(\frac{H_{p_o}}{7{,}600}\right) \tag{9}$$

For a complete model, in addition to Eq. 5, the energy balance equation introduced by Luikov (1966) is required. It describes heat transfer through a capillary porous medium and is given as:

$$\frac{\partial T}{\partial t} + \frac{1}{\rho C_T}\left(K_T\frac{\partial^2 T}{\partial x^2}\right) + \frac{E_b\lambda}{C_T}\left(\frac{\partial m}{\partial t}\right) \tag{10}$$

where m is the fractional moisture content expressed in grams of water per gram of oven-dry wood, and λ, called the condensation or evaporation criterion, is the ratio of the vapor diffusion coefficient in the material to the coefficient of total diffusion of moisture inside the material. Thus, λ defines the amount of transferable vapor in the body in relation to the total flow of moisture in the wet material. In this study, since moisture transfer occurred only by diffusion, without any liquid phase present, λ was set equal to one.

All other variables, as well as the moisture sorption isotherms required in the solution of Eqs. 5 and 10, were based on experimental data obtained in previous studies (Choong, 1962; Stamm, 1964). The corresponding functions for wood have been proven, in the past, to strongly depend on the moisture content and the temperature levels (Siau, 1984; Skaar, 1989). These functions are given in the Appendix A.

Method of Solution

The model equations are solved numerically. However, analytical solutions available for constant material properties and boundary conditions (Crank, 1975) have been compared with the numerical solution to establish the accuracy of the numerical procedure. The results are quite satisfactory and are presented in subsequent sections.

The model equations are solved using the method of lines. Since the model comprises a system of coupled parabolic partial differential equations, the method of lines is ideally suited (Machura and Sweet, 1980; Sincovec and Madsen, 1975) for this purpose. With this approach, the space variables are first discretized (in this case, using second-order accurate central differences), and the resulting system of ordinary differential equations (ODEs) is solved by an appropriate ODE solver. In this work, the Gear's (1971) backward differentiation scheme was used, as implemented in the subroutine DDRVB2, available at the Computer Software Libraries of the Los Alamos National Laboratory.

Considering variable mesh spacing, the appropriate second-order finite difference approximations of the spatial derivatives of a function f at a point i are:

$$\left(\frac{\partial f}{\partial x}\right)_i \cong \left(\frac{\delta f}{\delta x}\right)_i \equiv \frac{f_{i+1}-f_{i-1}}{\delta x_+ + \delta x_-} \tag{11}$$

and

$$\left(\frac{\partial^2 f}{\partial x^2}\right)_i \cong \left(\frac{\delta^2 f}{\delta x^2}\right) = b_i[c_i f_{i+1} - f_i + d_i f_{i-1}] \tag{12}$$

where, $b_i = 2/(\delta x_+)(\delta x_-)$, $c_i = \delta x/\alpha_i$, $d_i = \delta x_+/\alpha_i$, and $\alpha_i = \delta x_+ + \delta x_-$. In the above equations, δx_- and δx_+ indicate the mesh size to the left and to the right of the grid point i, respectively. Following the spatial discretization using N grid points, the model reduces to a set of 2*N nonlinear, coupled ODEs whose general form is:

$$\frac{dT_i}{dt} = f_1\left(P_i, \left(\frac{\delta^2 T}{\delta x^2}\right)_i, \left(\frac{dm_i}{dt}\right)\right) \tag{13}$$

and

$$\frac{dM_i}{dt} = f_2\left(P_i, \left(\frac{\delta T}{\delta x}\right)_i, \left(\frac{\delta M}{\delta x}\right)_i, \left(\frac{\delta^2 T}{\delta x^2}\right)_i, \left(\frac{\delta^2 M}{\delta x^2}\right)_i\right) \tag{14}$$

where P_i is, in general, a function of the material properties at the point i. This term will also include spatial derivatives of the physical properties of the system (expressed through derivatives such as $\delta D/\partial x$ or $\partial\phi/\partial x$, in Eq. 5).

Boundary conditions

The boundary conditions considered in this study are those of negligible heat- and mass-transfer resistances at the interface w, consistent with the intense aeration present in the drying chambers (air velocity approximately 5 m/s), and the thickness of the specimen (Avramidis and Siau, 1987a). It is assumed, therefore, that T_w and M_w are constant. At the axis of symmetry, a condition of zero flux is imposed:

$$\left(\frac{\partial T}{\partial x}\right)_s = 0 \text{ and } \left(\frac{\partial M}{\partial x}\right)_s = 0 \tag{15}$$

In the numerical implementation of the model, the partial derivatives on the axis of symmetry are approximated by the following one-sided second-order expression (Collatz, 1966):

$$\left(\frac{\partial^2 f}{\partial x^2}\right)_s \cong \frac{1}{(\delta x)^2}[2f_s - 5f_{s+2} + 4f_{s+2} - f_{s+3}] \times \left[+\frac{11}{12}\delta x^2\left(\frac{\partial^4 f}{\partial x^4}\right)_s\right] \tag{16}$$

where s, indicates values on the axis of symmetry.

Comparison with analytical solution

Under conditions of constant surface temperature and with constant diffusivity, the solution of the energy equation in one dimension is (Crank, 1975):

$$\frac{T-T_o}{T_i-T_o} = 1 - \frac{4}{\pi}\sum_{n=0}^{\infty}\frac{(-1)^n}{2n+1}\exp\left[\frac{-D_{hT}(2n+1)^2\pi^2 t}{4l^2}\right] \times \cos\left[\frac{(2n+1)\pi x}{2l}\right] \tag{17}$$

where t is the time, l is the thickness of the specimen, and x is the location within the specimen. This solution has been compared with the numerical solution of Eq. 10, excluding the evaporation term $(E_b\lambda/c_T)(\partial m/\partial t)$, and with constant thermal diffusivity (D_{hT}). Various mesh sizes and configurations have been employed in an attempt to choose the mesh that provides a balance between accuracy and computational cost. Meshes of constant size, as well as graded meshes, were used. The graded meshes were generated by a recursive formula of the type:

$$(\delta x)_n = \alpha(\delta x)_{n-1},\ n=2,\ N,\ 0<\alpha\leq 1 \tag{18}$$

Figure 1, shows the numerical solution to the energy equation

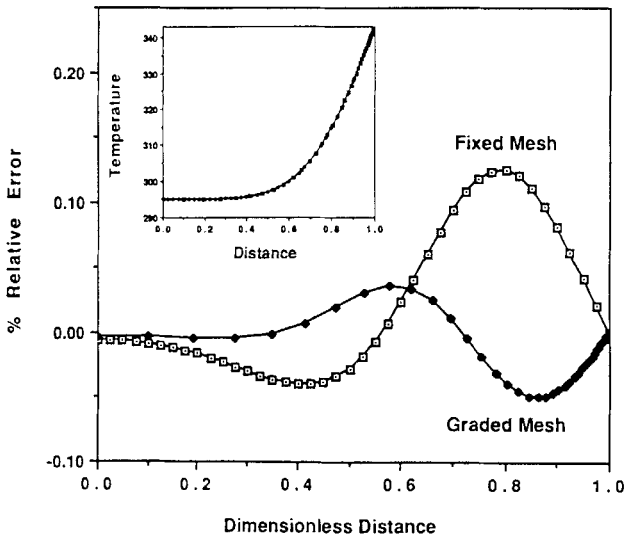

Figure 1. Numerical solution of the energy equation and the associated relative percent errors for two meshes: (a) uniform, and (b) graded.

with the constant coefficient ($D_{hT}=0.1$), at time $t=0.3$, along with the associated percent relative error, defined as $100(T_{num}-T_{anal})/T_{anal}]$, as a function of the dimensionless distance. T_{anal} is the analytical solution given by Eq. 17. The numerical solutions corresponding to the constant and graded meshes are practically identical. An examination of the percent relative error, however, indicates that the use of a graded mesh with 41 nodes, and spacing parameter α equal to 0.9, improves the accuracy of the numerical solution when compared with equidistant mesh of equal size. At the same time, a graded mesh provides a better resolution of the thermal gradients near the surface. Based on this experience, a graded mesh of 41 nodes and an $\alpha=0.9$ was used in all the calculations reported in this study.

Experimental Procedure

A rectangular ($40\times100\times200$ mm), all-heartwood specimen of Douglas fir (*Pseudotsuga menziessi* (Poir.) Britton), was cut from a piece of green lumber. The specimen was initially oven-dried at 103 ± 2°C until the weight became constant, and then it was placed in a conditioning chamber that was set to 20°C and 90% relative humidity, corresponding to an equilibrium moisture content of 20%, approximately. The air velocity in the chamber was maintained at 5 m/s. The conditioning process continued until no detectable weight change had occurred for 48 hours.

When it reached equilibrium, the specimen was immediately placed in a plastic bag and stored in a controlled environment room at 20°C. Concurrently, the conditions in the chamber were changed to 70°C and 50% relative humidity, resulting in an equilibrium moisture content of approximately 5%. When the chamber attained the new conditions, the specimen was immediately transferred back to the chamber and the change of temperature at its geometric center was monitored with time by a copper-constantan type T, teflon-insulated thermocouple that was connected to a data logger. At the same time, the change in the specimen's weight with time, was monitored with

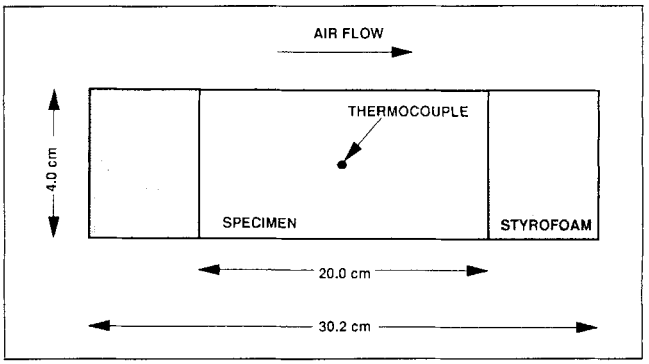

Figure 2. Cross section of the wood-styrofoam experimental assembly.

a digital balance. Since the weight monitoring required the removal of the specimen from the chamber, efforts were made for this to be done as fast as possible, thus minimizing any sorption interruptions.

Heat and moisture transfer took place along the specimen's thickness (radial direction, 40 mm) through the top and bottom surfaces. To accomplish this, the specimen's sides were covered flush by thick styrofoam. Moreover, the sides of the specimen were sealed with epoxy resin and rubber sheets to provide thermal insulation and prevent moisture loss. The styrofoam-specimen assembly is shown in Figure 2.

When there was no detectable weight change of the styrofoam-specimen assembly for 48 hours, it was assumed that a state of equilibrium was reached, and that the experimental run had been completed. At that point, the specimen was immediately removed from the styrofoam block, and a 1-cm-thick cross section was cut with a band saw. The section was then cut into seven slices that were immediately weighed. Then they were placed in a forced-circulation oven for 24 hours at 103 ± 2°C, thus obtaining the final moisture profile along the thickness of the specimen. Moisture profiles during desorption were not measured because there currently is no technique with which to measure these profiles in a rapid and nondestructive manner.

Results and Discussion

In this section, we present a simulation of the desorption experiment outlined in the previous section. The specimen as can be seen in Figure 2, had a length to half-thickness ratio of 10. Because of this, and because the specimen's sides were covered with epoxy and styrofoam, it was reasonable to assume that heat and mass transfer occurred predominantly in the thickness direction (perpendicular to the direction of the air flow). Hence, the system was modeled as one-dimensional. This assumption is expected to be most valid at the geometrical center of the specimen where the thermocouple was located, and therefore its temperature measurements were not expected to be influenced by end (or two-dimensional) effects. Two-dimensional effects might, however, affect the moisture transfer and the total desorption time, even though previous experience suggests that transport in specimens of this configuration can be safely approximated as one-dimensional (Stanish et al., 1986). Additionally, because of the high air velocities (5 m/s) in the drying chamber, the boundary con-

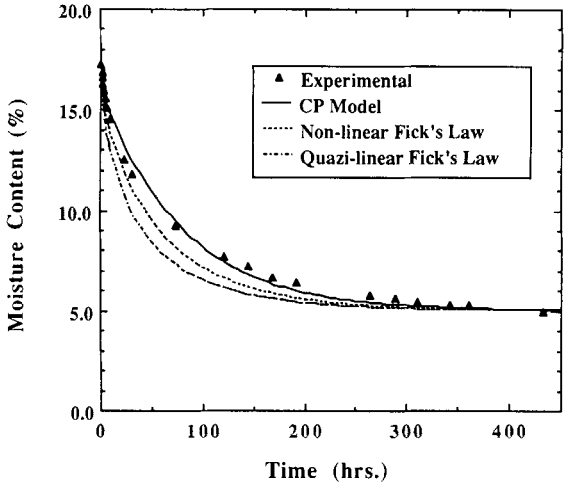

Figure 3. Plot of experimental and predicted average moisture content by the CP models and Fick's equations.

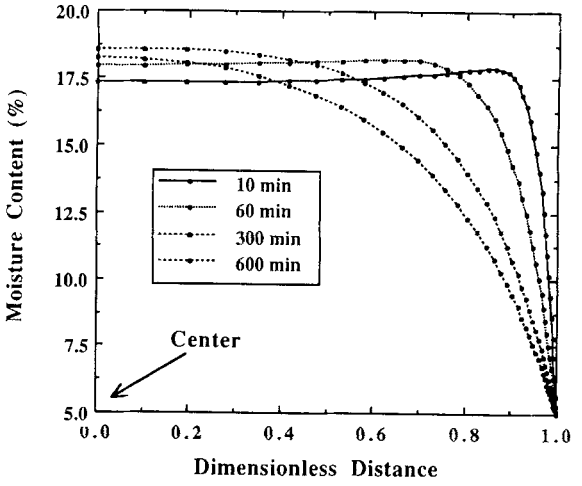

Figure 4. Moisture content profiles predicted by the CP model.

ditions of negligible heat- and mass-transfer resistance employed at the wood/air interface are physically realistic.

The desorption curve

Figure 3 is a comparison of the experimental and predicted overall average moisture content within the desorbing specimen as a function of time. The conditions supplied to the computer model correspond to the experiment outlined in the previous section. As can be seen, the predictions of the CP model are in excellent agreement with the experimental desorption curve. This establishes the validity of the proposed CP model in quantitatively predicting the desorption process in complex porous hygroscopic materials.

The impact of the thermal gradient on the moisture flux is eliminated by setting ϕ equal to zero in Eq. 5. The resulting expression is equivalent to the one-dimensional Fick's second law of diffusion for a material whose diffusion coefficient is a strong function of temperature and moisture content:

$$\frac{\partial M}{\partial t}=D\left(\frac{\partial^2 M}{\partial x^2}\right)+\frac{\partial D}{\partial M}\left(\frac{\partial M}{\partial x}\right)^2+\left(\frac{\partial D}{\partial T}\frac{\partial M}{\partial x}\frac{\partial T}{\partial x}\right) \qquad (19)$$

It is of interest to investigate how Eq. 19 compares with the proposed CP model and the experimental data. This comparison is also presented in Figure 3, where the predicted curve is under the name of nonlinear Fick's law. As can be seen, it lies significantly below the curve predicted by the CP model (since no thermal counter-diffusion is allowed to occur in the Fickian model), but, evidently, it is a reasonable approximation to the experimental desorption curve at least for the initial stage of drying. The drying curve seems to be a strong function of the diffusion coefficient itself, as can be seen by observing the dotted-broken line in Figure 3. This line was obtained by solving a quasi-linear form of the Fickian model, such as:

$$\frac{\partial M}{\partial t}=D(T, M)\frac{\partial^2 M}{\partial x^2} \qquad (20)$$

derived from Eq. 19, in which the derivatives $\partial D/\partial M$ and $\partial D/\partial T$ were set equal to zero but in which the diffusivity was still a function of temperature and moisture content given by the appropriate function in the Appendix A. It is obvious that this model further under predicts the drying time. Clearly, the drying of porous hygroscopic materials as complex as wood is a highly nonlinear process and this nonlinearity needs to be preserved in the models if meaningful quantitative predictions are to be made.

Internal distribution of moisture and temperature

It has been shown that the proposed CP model can quantitatively predict the macroscopic moisture diffusion during desorption with satisfactory accuracy. A further examination of the internal distribution of moisture that was predicted by the CP model, and by the nonlinear Fickian model reveals significant quantitative as well as qualitative differences. Figure 4 shows the moisture profiles within the specimen, as predicted by the CP model for the first 10 hours of the experimental run, where the moisture at the surface immediately takes the ambient value of 5% as a result of zero mass transfer resistance condition at the wood/air interface.

Initially, the center remains at the original 17.3% and there is a local maximum in moisture content just below the surface. As desorption progresses, this maximum shifts towards the center and the slope of the moisture profile becomes smaller. Concurrently, the center's moisture content increases. This trend continues until well into the 600 minute time period during which the moisture content of the center reaches approximately 18.3%. Beyond that point, the moisture content continuously decreases until final equilibrium. This diffusion of moisture from the surfaces to the center resulted from the steep thermal gradient that existed across the thickness of the specimen in the initial stages of drying.

This transient distribution of moisture can have a significant effect on the internal stresses that develop during the first stages of desorption because of the differential thermal and/or hydro expansion (contraction) of the material. It was speculated in the past that large temperature gradients could result in thermal diffusion (Soret effect) and establish a moisture flux toward

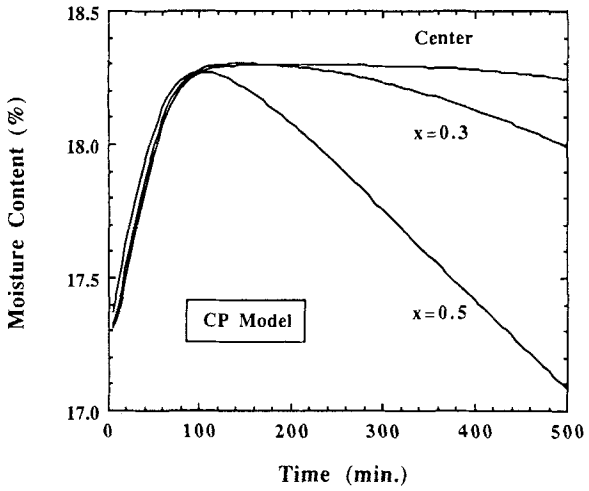

Figure 5. Changes of moisture content with time at three locations inside the specimen.

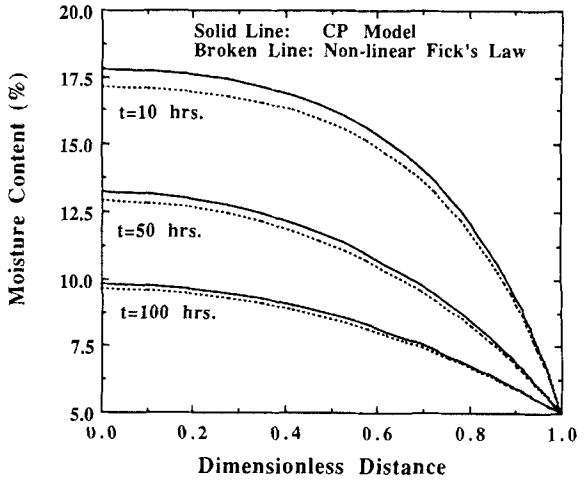

Figure 7. Predicted moisture profiles by the CP model and Fick's law (long times).

the center of the specimen under unsteady-state conditions (Siau, 1983a). As a result, the moisture could increase in the center of the specimen during the initial stages of desorption. The existence of this phenomenon has been proven experimentally under steady-state nonisothermal conditions in the past (Avramidis and Siau, 1987b; Avramidis et al., 1987). The present study has predicted the existence of a transient Soret effect even though experimental validation is not possible because of the instrumentation difficulties associated with the required nondestructive measurements.

The prediction of the Soret effect is more evident in Figure 5, where the predicted moisture contents of the center and two other locations along the thickness of the specimen are plotted against time. The initial increases and later decreases of moisture content are very prominent. Figure 6, shows the differences between the CP model and Fick's law in predicting the existence of the Soret effect during unsteady-state nonisothermal desorption in small times. Clearly, in contrast to the CP model, no transient moisture content rise in the core of the specimen is predicted by Fickian diffusion. The corresponding internal moisture distributions at longer times are shown in Figure 7. It is evident that the Soret effect becomes less significant as time progresses, and, therefore, the form of ϕ becomes less meaningful. At long times, moisture profiles could well be simulated by Fick's second law of diffusion.

The predicted temperature profiles within the specimen during drying are shown in Figure 8 for both the CP model (solid lines), and the nonlinear Fickian model (dotted lines). It is evident that thermal equilibrium within the specimen is reached much faster than moisture equilibrium. Furthermore, the interactions between mass and heat transfer are demonstrated by the fact that the CP model predicts higher temperatures at the core of the specimen than the Fickian model, probably as a result of the Soret effect. Finally, Figure 9 shows a comparison between the experimental and predicted temperatures at the center of the specimen during desorption. A close examination of the graph reveals that both models predict the same temperature for the first 30 minutes. It is also noticed

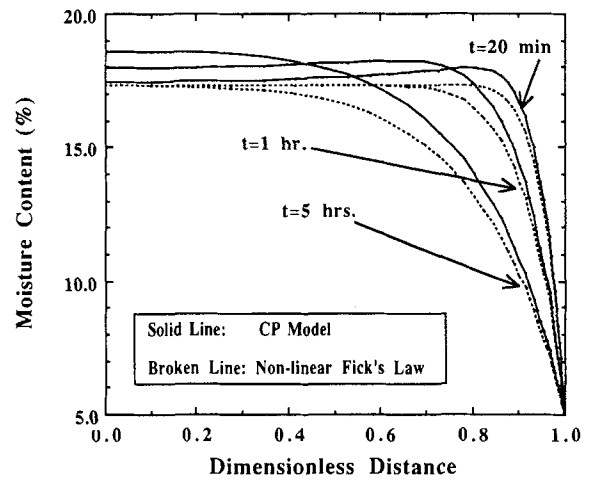

Figure 6. Predicted moisture profiles by the CP model and Fick's law (short times).

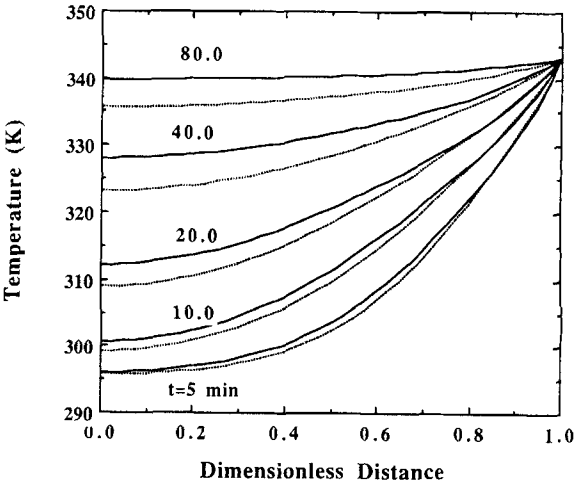

Figure 8. Predicted temperature profiles within the specimen by the CP (solid line) and the Fickian model (dotted line).

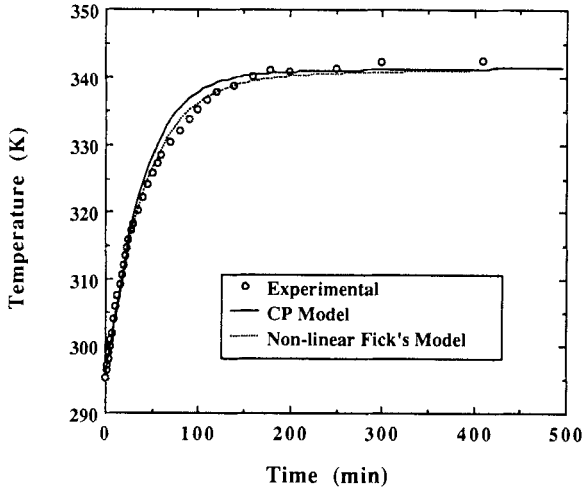

Figure 9. Plot of experimental and predicted values for the temperature at the specimen's center vs. time.

that the CP model predicts a slightly higher temperature for the next 120 minutes, a difference that subsequently diminishes. Overall however, it is evident from the graph that theory and experiment are in very close agreement.

Conclusions

A model that predicts heat and moisture transfer in a nonhomogeneous hygroscopic material such as wood, was evaluated using unsteady-state nonisothermal diffusion experimental data. The proposed model provides an excellent prediction of the specimen's average moisture content during desorption, thus establishing its validity. A very good agreement was also found between the predicted and experimental temperature rise data in the specimen's center. The model also predicted moisture flow from the surface toward the center of the specimen during the initial stages of the desorption process, indicating the existence of the Soret effect. A comparison of the moisture predictions by the proposed model to the two forms of Fick's second law equation revealed the inability of the latter to accurately predict both the drying curve and the thermal-diffusion phenomenon.

It is concluded, therefore, that the proposed model, which utilizes the chemical potential gradient of water as the driving force for diffusion, has been very successful in simulating moisture desorption in the hygroscopic range of wood under nonisothermal unsteady-state conditions.

Acknowledgment

This project was financially supported by a Natural Sciences and Engineering Council of Canada operating grant (OGP 0036755). Work performed at Los Alamos National Laboratory was sponsored by the Office of the Director and the Mechanical and Electronics Engineering Division (MEE), Los Alamos National Laboratory.

Notation

c_T = specific heat of wood, cal/g·K
D = transverse diffusion coefficient, cm²/s
D_{hT} = transverse thermal diffusivity coefficient, cm²/s
E_b = activation energy, cal/mol
E_o = heat of vaporization, cal/mol
E_l = differential heat of sorption, cal/mol
G = specific gravity
H = relative humidity, %
K_M = coefficient for diffusion due to moisture gradient, g/cm·s %
K_T = transverse thermal conductivity coefficient, cal/cm·K·s
M = moisture content (oven dry basis), %
P_o = saturated vapor pressure at T, cm Hg
R = universal gas constant, (=2 cal/mol)
t = time, s
T = temperature, K
x = distance, cm
V_a = porosity of wood

Greek letters

μ^o = chemical potential of saturated vapor, cal/mol
ρ = density, g/cm³
λ = condensation or evaporation criterion (= 1)

Literature Cited

Adesanya, B. A., A. K. Nanda, and J. N. Beard, "Drying Rates during High Temperature Drying of Yellow Poplar," *Drying Technol.*, **6**(1), 95 (1988).

Avramidis, S., and J. F. Siau, "An Investigation of the External and Internal Resistance to Moisture Diffusion in Wood," *Wood Sci. Technol.*, **21**, 249 (1987).

Avramidis, S., and J. F. Siau, "Experiments in Nonisothermal Diffusion of Moisture in Wood," Part 3. *Wood Sci. Technol.*, **21**, 329 (1987).

Avramidis, S., N. Kuroda, and J. F. Siau, "Experiments in Nonisothermal Diffusion of Moisture in Wood. Part II," *Wood Fiber Sci.* **19**(4), 407 (1987).

Barbour, J. R., and J. A. Johnson, "A Microstructrally Based Model for Moisture Movement in Wood Below the Fiber Saturation Point," *Wood Drying Symposium*, pp. 247–254, F. Kayihan, J. A. Johnson, and R. W. Smith, eds., IUFRO, Seattle, WA (1989).

Beard, J. N., H. N. Rosen, and B. A. Adesanya, "Temperature Distributions and Heat Transfer during the Drying of Lumber," *Drying Tech.*, **1**(1), 117 (1983).

Blondin, H. P., J. C. David, J. M. Vergnaud, J. P. Illien, and M. Malizewicz, "Modeling the Drying Process of Coatings with Various Layers," *J. Coatings Technol.*, **59**(746), 27 (1987).

Bramhall, G., "Mathematical Model for Lumber Drying. I. Principles Involved," *Wood Sci.*, **12**(1), 14 (1979).

Bramhall, G., "Mathematical Model for Lumber Drying. II. The Model," *Wood Sci.*, **12**(1), 22 (1979).

Choong, E. T., "Movement of Moisture Through Softwood (Abies sp) in the Hygroscopic Range," PhD Thesis, State Univ. of New York, College of Environmental Sci. and Forestry, Syracuse, N.Y. (1962).

Collatz, L., *The Numerical Treatment of Differential Equations*, Springer-Verlag (1966).

Collins, T. A., "The Use of Resin Hybrids to Control Moisture Absorption in Fibre-Reinforced Plastics," *Composites*, **22**(5), 369 (1991).

Crank, J., *The Mathematics of Diffusion*, Clarendon Press, Oxford (1975).

Croll, S. G., "Heat and Mass Transfer in Latex Paints During Drying," *J. of Coatings Technol.*, **59**(751), 81 (1987).

DeGroot, R. S., and P. Mazur, *Nonequilibrium Thermodynamics*, North-Holland Pub. Co. (1962).

Droin, A., J. L. Taverdet, and J. M. Vergnaud, "Modeling the Kinetics of Moisture Adsorption by Wood," *Wood Sci. Technol.*, **22**, 11 (1988).

Droin-Josserand, A., J. L. Taverdet, and J. M. Vergnaud, "Modelling the Absorption and Desorption of Moisture of Wood in an Atmosphere of Constant and Programmed Relative Humidity," *Wood Sci. Technol.*, **22**, 299 (1988).

Droin-Josserand, A., J. L. Taverdet, and J. M. Vergnaud, "Modelling

the Process of Moisture Absorption in Three Dimensions by Wood Samples of Various Shapes: Cubic, Parallelepipedic," *Wood Sci. Technol.*, **23**, 259 (1989).
Droin-Josserand, A., J. L. Taverdet, and J. M. Vergnaud, "Modelling of Moisture Adsorption within a Section of Parallelepipedic Sample of Wood by Considering Longitudinal and Transversal Diffusion," *Holzforschung*, **43**(5), 297 (1989).
Fortes, M., and M. R. Okos, "A Non-Equilibrium Thermodynamic Approach to Transport Phenomena in Capillary Porous Media," *Proceedings First International Drying Symposium*, A. S. Mujumdar, ed., Montreal, pp. 100–109 (1978).
Gear, C. W., *Numerical Initial Value Problems in Ordinary Differential Equation*, Prentice-Hall (1971).
Haghighi, K., J. Irudayaraj, R. L. Stroshine, and S. Sokhansanj, "Grain Kernel Drying Simulation using the Finite Element Method," *Am. Soc. Agr. Eng.*, **33**(6), 1957 (1990).
Jomma, W., and J. R. Puiggali, "Drying of Shrinking Materials: Modelling with Shrinkage Velocity," *Drying Technol.*, **9**(5), 1271 (1991).
Kayihan, F., *Adaptive Optimal Scheduling and Control of Batch Lumber Kilns using a Population Balance Model*, A. S. Mujumdar, ed., *Drying '86*, pp. 391–400 (1986).
Laubi, S., and J. M. Vergnaud, "Effect of Temperature on the Transfer Between Epoxy Coating and Water," *European Polymer J.*, **27**(12), 1425 (1991).
Lewis, R. W., M. Strada, and G. Comini, "Drying Induced Stresses in Porous Bodies," *Int. J. Num. Meth. Engr.*, **11**, 1175 (1977).
Lui, J. Y., "Lumber Drying in a Medium with Variable Potentials," *General Papers: Phase Change and Convective Heat Transfer: Proceedings of AIAA/ASME Thermophysics and Heat Transfer Conference*, Seattle, WA, K. Vafai, et al., eds., pp. 149–156 (1990).
Luikov, A. V., *Heat and Mass Transfer in Capillary-Porous Bodies*, Pergamon Press, Oxford (1966).
Machura, M., and R. A. Sweet, "A Survey of Software for Partial Differential Equations," *ACM Trans. Math. Software*, **6**, 461 (1980).
Maffetone, P. L., G. Astarita, L. Cori, L. Carnelli, and F. Balestri, "Slit Devolatilization of Polymers," *AIChE J.*, **37**(5), 724 (1991).
Nelson, R. M. Jr., "Diffusion of Bound Water in Wood. Part I: The Driving Force," *Wood Sci. Technol.*, **20**, 125 (1986).
Nelson, R. M. Jr., "Diffusion of Bound Water in Wood. Part 2: A Model for Isothermal Diffusion, *Wood Sci. Technol.*, **20**, 235 (1986).
Nelson, R. M. Jr., "Diffusion of Bound Water in Wood. Part 3: A Model for Nonisothermal Diffusion," *Wood Sci. Technol.*, **20**, 309 (1986).
Oliveira, A. O., and O. E. Fernandes, "Simulation of the Convective Drying of Capillary-Porous Materials," *Drying '86*, A. S. Mujumdar, ed., pp. 65–70 (1986).
Oriani, R. A., "Delineation of the Problem of Soret Diffusion," *J. Chem. Phys.*, **34**(5), 1773 (1961).
Parry, J. L., "Mathematical Modelling and Computer Simulation of Heat and Mass Transfer in Agricultural Grain Drying: A Review," *J. Agric. Eng. Res.*, **32**, 1 (1985).
Parrauffe, J. M., and A. S. Majumdar, "Bibliography on Mathematical Models of Drying and Dryers," *Drying Technol.*, **6**(2), 302 (1988).
Phillips, J. R., and D. A. DeVries, "Moisture Movement in Porous Materials Under Temperature Gradients," *Trans. Am. Geophys. Union.*, **38**(2), 222 (1957).
Perre, P. S., Ben Nasrallah, and G. Arnaud, "A Theoretical Study of Drying: Numerical Simulations Applied to Clay-Brick and Softwood," A. S. Mujumdar, ed., *Drying '86*, pp. 382–390 (1986).
Plumb, O. A., C. A. Brown, and B. A. Olstead, "Experimental Measurements of Heat and Mass Transfer during Convective Drying of Southern Pine," *Wood Sci. Technol.*, **18** 187 (1984).
Prigogine, I., *Introduction to Thermodynamics of Irreversible Processes*, Interscience Publishers, (1961).
Siau, J. F., "Nonisothermal Moisture Movement in Wood," *Wood Sci.*, **13**(1), 11 (1980).
Siau, J. F., "A Proposed Theory for Nonisothermal Unsteady-State Transport of Moisture in Wood," *Wood Sci. Technol.*, **17**, 75 (1983).
Siau, J. F., "Chemical Potential as a Driving Force for Nonisothermal Moisture Movement in Wood," *Wood Sci. Technol*, **17**, 101 (1983).
Siau, J. F., "Chemical Potential and Nonisothermal Diffusion. Letter to the Editor," *Wood Fiber Sci.*, **16**(4), 628 (1984).
Siau, J. F., *Transport Processes in Wood*, Springer-Verlag, New York (1984).
Siau, J. F., and S. Avramidis, "Application of a Thermodynamic Model to Nonisothermal Diffusion Experiments," *Wood Sci. Technol.*, in press 1992.
Siau, J. F., F. Boa, and S. Avramidis, "Experiments in Nonisothermal Diffusion of Moisture in Wood," *Wood Fiber Sci.*, **18**(1), 84 (1986).
Sincovec, R. F., and N. K. Madsen, "Software for Nonlinear Partial Differential Equations," *ACM Trans. Math. Software*, **1**(3), 232 (1975).
Skaar, C., *Wood-Water Relations*, Springer-Verlag, New York (1989).
Stamm, A. J., *Wood and Cellulose Science*, Ronald New York (1964).
Stanish, M. A., G. S. Schajer, and F. Kayihan, "Mathematical Modeling of Wood Drying from Heat and Mass Transfer Fundamentals," A. S. Mujumdar, ed., *Drying '84*, pp. 360–367.
Stanish, M. A., G. S. Schajer, and F. Kayihan, "A Mathematical Model of Drying for Hygroscopic Porous Media," *AIChE J.*, **32**(8), 130 (1986).
Strongin, V., and I. Border, "Analytical Prediction of Drying Rate Curves," A. S. Mujumdar, ed., *Drying '86*, pp. 112–118 (1986).
Thomas, H. R., R. W. Lewis, and K. Morgan, "An Application of the Finite Element Method to the Drying of Timber," *Wood and Fiber*, **11**(4), 237 (1980).
Vernaud, J. M., "Liquid Transport Processes in Polymeric Materials: Modelling and Industrial Applications," Prentice Hall, Englewood Cliffs, N.J. (1991).

APPENDIX

The diffusion coefficient for gross wood in the direction transverse to the longitudinal (fiber) axis is given by:

$$D = 0.07 \exp[-(9{,}200 - 70M/RT]/(1 - V_a)\ (1 - \sqrt{V_a})$$

where V_a is the porosity of the material given by the empirical equation:

$$V_a = 1 - 0.46(0.667 + 0.01M]$$

The thermal diffusivity for wood is given by:

$$D_{hT} = K_T / c_T \rho$$

where K_T is the thermal conductivity coefficient for wood which can be calculated by the empirical equation:

$$K_T = [0.45(5.18 + 0.096M) + 0.57 V_a]E - 4$$

and c_T and ρ are the specific heat and density of wood, respectively, as given:

$$c_T = (-0.0323 + 0.0011T + 0.01M)/(1 + 0.01M)$$

$$\rho = 0.46(1 + 0.01M)$$

The derivative of the water chemical potential with respect to temperature as well as the water activation, vaporization and differential energies required in Eq. 9, are given by:

$$d\mu^o/dT = 10.37 + 0.0077\,(T - 273)$$

$$E_o = 10{,}730 + 10(273 - T)$$

$$E_o = 9{,}200 - 70M$$

$$E_L = 5{,}000 \exp(-0.14M)$$

The slope of the sorption isotherm is given by:

$$\partial M/\partial H = (A + CH^2)/(A + BH - CH^2)^2$$

where

$$A = (W/18)[1/K_2(K_1 + 1)]$$

$$B = (W/1{,}800)[(K_1 - 1)/(K_2 + 1)]$$

$$C = (WK_1K_2)/[180{,}000(K_1 + 1)]$$

$$W = 1591 - 9.4T + 0.0185T^2$$

$$K_1 = -49.74 + 0.32T - 0.000501T^2$$

$$K_2 = -0.176 + 0.001697T - 5.64E - 6T^2$$